JOURNAL OF SPACECRAFT AND ROCKETS
Vol. 35, No. 2, March–April 1998

Local Environment Surrounding the Midcourse Space Experiment Satellite During Its First Week

B. D. Green,* G. E. Galica,† and P. A. Mulhall‡
Physical Sciences, Inc., Andover, Massachusetts 01810
O. M. Uy,§ J. C. Lesho,¶ M. T. Boies,** R. C. Benson,†† T. E. Phillips,‡‡ D. M. Silver,†† and R. E. Erlandson§§
Johns Hopkins University, Applied Physics Laboratory, Laurel, Maryland 20723
B. E. Wood¶¶
Sverdrup Technology, Inc., Arnold Air Force Base, Tennessee 37389
D. F. Hall***
The Aerospace Corporation, Los Angeles, California 90009
and
J. D. Mill†††
Environmental Research Institute of Michigan, Arlington, Virginia 22209

The environment measured surrounding the complex Midcourse Space Experiment spacecraft during its first week on orbit is reported. A suite of instruments including a pressure sensor, a neutral and an ion mass spectrometer, quartz crystal microbalances, and flashlamp-based water and particle detectors were activated within hours after launch. These instruments measured the gaseous composition, particulate, and film accretion temporal histories. Spacecraft environment cleanliness and response to operational activities were used to guide decisions about sensor operation. As a result of careful material selection and ground preparation procedures, the measured levels of condensible species were sufficiently low to permit safe sensor operation after only a few days in orbit.

Introduction

THE Midcourse Space Experiment (MSX) spacecraft is designed to precisely measure the optical signatures from a broad range of natural phenomena (the Earth, its upper atmosphere, and celestial objects) as well as from man-made targets. These scenes are observed with a suite of fully characterized, carefully calibrated, very sensitive optical instruments with broad spectral imaging capability. Optical measurements spanning from the far-ultraviolet (UV) (110 nm) to the very long-wavelength infrared (IR) (28 μm) spectral regions are performed in a series of systematic measurement sequences. High sensitivity in the long-wavelength IR is achieved by cryogenically cooling the IR focal planes and mirrors to below 20 K by thermal conduction from a cryostat containing solid hydrogen. A releasable solid argon-cooled door covered the evacuated telescope and optical assembly. The mission objectives and instrumentation have been described.[1,2] The designed mission lifetime is four years. This sophisticated spacecraft is 5.1 m long and 1.5 m square and weighs ≈2700 kg. Most of the external surfaces of MSX are covered with multilayer insulation (MLI) composed of 20 layers of aluminized Mylar® separated by Dacron® netting. The innermost surface and exterior layers have beta cloth or silver Teflon® with indium tin oxide surface coating.[3] The MSX spacecraft with optical and contamination instrument locations indicated is shown in Fig. 1. The MSX spacecraft was launched from Vandenburg Air Force Base into a circular, 99-deg, near sun-synchronous, 904-km-altitude orbit by a Delta II booster on April 24, 1996, at 12:27 Greenwich mean time (Eastern daylight savings time plus 4 h).

Contamination could cause degradation in the performance of these sensitive optical instruments, invalidating all of the careful prelaunch preparation and calibration. Absorption by nanometer thicknesses of organic molecular films on UV optics and micrometer-scale ices of nearly all gases on the cryogenic IR optics will cause these mirrors to lose throughput or increase scatter by orders of magnitude. Attitude maneuvering is achieved with reaction wheels to eliminate thrust exhaust contamination effects. The most frequent spacecraft attitude is with its $+Z$ face into the velocity vector and the electronics section facing nadir. To help ensure the desired operational performance, a thorough contamination-control plan for material selection and handling was also implemented. Furthermore, a suite of contamination instruments is included in the manifest to monitor performance during ground processing and integration. Contamination modeling activities[3] accompanied all phases of the development of MSX, providing an understanding of measurable quantities and prediction of expected environments.

The MSX external contamination model[3,4] predicts molecular, particulate, and electromagnetic effects with the source terms based on the MSX contamination control plan and laboratory[5] and flight measurements. Transport, deposition, and the effects produced are also modeled. This model provides detailed predictions and creates the essential linking of each contamination sensor's observations.

Instrument Suite and Experiments

Molecular species concentrations, deposited film thicknesses, particle occurrence above surfaces, and spacecraft charging are all

Received Feb. 19, 1997; revision received Sept. 19, 1997; accepted for publication Sept. 21, 1997.

* Vice President, 20 New England Business Center. Senior Member AIAA.
† Senior Scientist, 20 New England Business Center. Member AIAA.
‡ Senior Programmer, 20 New England Business Center.
§ Principal Staff Chemist, Technical Services Department, 11100 Johns Hopkins Road. Member AIAA.
¶ Senior Staff Engineer, Technical Services Department, 11100 Johns Hopkins Road.
** Senior Staff Engineer, Space Department, 11100 Johns Hopkins Road. Member AIAA.
†† Principal Staff Chemist, Applied Research and Technology Department, 11100 Johns Hopkins Road. Member AIAA.
‡‡ Senior Staff Chemist, Applied Research and Technology Department, 11100 Johns Hopkins Road. Member AIAA.
§§ Senior Staff Physicist, Space Department, 11100 Johns Hopkins Road. Member AIAA.
¶¶ Engineering Specialist, Operations Group, Arnold Engineering Development Center. Associate Fellow AIAA.
*** Research Scientist, Materials Group, P.O. Box 92957. Senior Member AIAA.
††† Chief Scientist, MSX, c/o Photon Research Associates, 1911 N. Ft. Myer Drive.

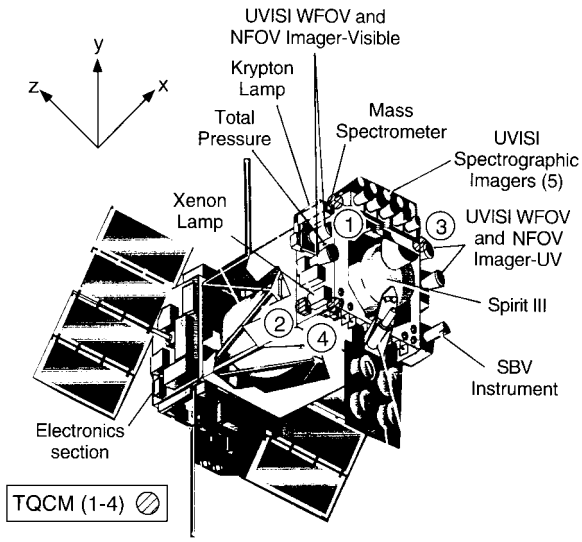

Fig. 1 Orbital configuration of the MSX spacecraft: WFOV, wide field of view; NFOV, narrow field of view; and SBV, space-based visible.

monitored. The contamination instruments (Ref. 6 provides detailed descriptions) include 1) a total pressure sensor (TPS) covering the range 10^{-5} to $< 10^{-10}$ torr and pointing in the same direction as the primary optical sensors ($+X$); 2) a closed-source quadrupole mass spectrometer for neutral molecules (NMS) with electron impact detection, covering masses 1–150 with 1-amu resolution, and a sensitivity of $\approx 10^5$ per cm^3, also pointing into $+X$; 3) a krypton flashlamp water sensor (KRF) to specifically monitor water densities above 10^7/cm^3 at meter distances above surfaces on the $+X$ instrument deck; 4) a Bennett radio frequency (RF) ion mass spectrometer (IMS) measuring masses 1–64 with sensitivity of ≈ 10 ions per cm^3, pointing in the $+Z$ direction; 5) four temperature-controlled quartz crystal microbalances (TQCMs) operated at -43 to -50°C (to sense deposited molecular films with sensitivities to detect 0.01-nm film thicknesses) located at different positions around the instrument section of MSX facing largely $-X$, $+X$, $+Z$, and $-Z$ (Ref. 7); 6) another QCM operated at near 20 K [cryogenic temperature-controlled QCM (CQCM)], located near the IR sensor primary mirror to monitor all species frozen onto cryogenic optical surfaces with 0.02-nm sensitivity; and 7) a xenon flashlamp particle illuminator (XEF) to illuminate particles in a volume 2 m above the $+X$ face of the instrument deck surfaces operating in concert with a visible 10×13 deg wide-field visible imager (IVW) to enable micrometer-diameter particle detection. In addition, the primary sensors—the UV visible imagers and spectrographic imagers (UVISI) with wide (10×13 deg) and narrow (1.32×1.6 deg) fields of view in the UV and visible, as well as the spatial IR imaging telescope (SPIRIT) III radiometers[1] sweeping across at 1×3 deg field of regard—will also be very sensitive detectors of spacecraft-produced particles as small as 0.1 and 10 μm, respectively.[8]

These instruments can operate individually but, by acting in concert during planned data collection events, their data can provide insight into the entire local environment. Experiment plans include brief periodic surveys of the environment, experiments to identify trends, experiments to discriminate the effects of discrete events, and experiments to measure the Earth's upper-atmospheric composition and variability. Because the instruments observe both spacecraft surfaces and space, they are able to observe the ambient atmosphere, direct outgassing flux from surfaces, and molecules scattered by collisions with contaminant and ambient molecules (return flux).

The early-time spacecraft environment will be dominated by release of material from ground and ascent operations (materials outgassing and venting, particle release). These effects are expected to decay with time on orbit. At later times, orbital production processes (abrasion from operations, thermal stresses and erosion) will dominate the near-spacecraft environment.

As part of their longer-duration measurements, the MSX contamination instruments will assess the effectiveness of contamination control procedures on the ground, monitor temporal trends, and quantify the effects of spacecraft operations on the local environment. The MSX contamination instruments will perform long-duration (multiyear) measurements of the spacecraft-induced effects, identifying sources and validating the model and contamination-control plan. This information will provide guidance to the designers and operations planners of future spacecraft.

This paper reports the environment observed surrounding the MSX spacecraft during its first week in orbit. The contamination instruments quantitatively measured accumulation, pressure history, and composition. We report the observed particulate occurrence rates and scattering radiance levels. The level of interference with the observation of far-field phenomena is also presented, along with an assessment of the level of spacecraft cleanliness. This information assisted in operational decisions about the safety of opening covers.

The primary optical sensors and contamination instruments were assembled, tested, and integrated under carefully controlled conditions.[9] Contamination control was an integral part of the MSX program. Design, materials selection, multiple-instrumented bakeouts, ground assembly, handling, and bagging all addressed contamination concerns. Visual and tape-lift inspections were performed frequently. Cleaning (vacuum and alcohol wipe) was performed as required. In spite of the multiple-year assembly process, the spacecraft external surfaces were measured to have an areal coverage by particles of 0.043 with no measurable molecular films before launch. On the pad, several adverse conditions arose during servicing and closeout. Owing to the necessity of frequent cryogenic servicing, activity-induced particulate redistribution was a concern. Procedures were developed, and levels were monitored frequently. Cooperation of all involved resulted in successful contamination control during ground operations.

Early Operations Period Contamination Environment Trends

During the first week in orbit, an extensive checkout procedure was followed for the spacecraft mechanical, power, data, telemetry, attitude, and optical sensor systems. The early operations events were conducted in a sequence that minimized the potential for contamination by performing the most potentially contaminating events first or by beginning operation of the instruments most sensitive to contamination after most contamination-producing spacecraft events were completed. Cover-opening advisory levels, based on contamination instrument measured values, were developed before launch. For the carefully calibrated, high off-axis-rejection optical systems on MSX, scatter by primary mirrors and optical throughput are very sensitive to degradation by contamination. The SPIRIT III primary mirror operating at temperatures near 20 K would condense nearly all molecular species (such as H_2O, CO_2, O_2, N_2, and Ar) likely to be encountered. Laboratory data have shown that deposited films of these species on optics at these temperatures produce negligible degradation in scatter performance at a wavelength of 10.6 μm, representative of the SPIRIT III spectral region, for film thicknesses smaller than 1 μm (Ref. 10). The primary mirrors of the UV instruments operate at 250–265 K, and volatile organics from outgassing are the likely deposition species. Even films of nanometer thicknesses will attenuate the UV transmission significantly. The external contamination model was used to correlate TPS, NMS, KRF, and TQCM measurements at the time of each door-opening decision to predict potential for performance degradation in the limits of both a constant and a decaying external pressure environment.

Any particles present on the primary mirrors will also significantly increase off-axis scattering. Mechanical operations were expected to be transient sources of particles. The contamination team recommended a sequence for these operations to minimize the impact of particulate contamination. On-orbit contamination instrument data, when linked with the model, permitted us to determine whether the spacecraft local environment permitted covers to be opened safely. Data from the contamination instrument suite allowed informed operations decisions to be made.

The contamination instruments were among the first to undergo checkout, permitting their early time monitoring of the spacecraft environment and the response of the environment to operations. Within 24 h after launch, all of the contamination instruments were

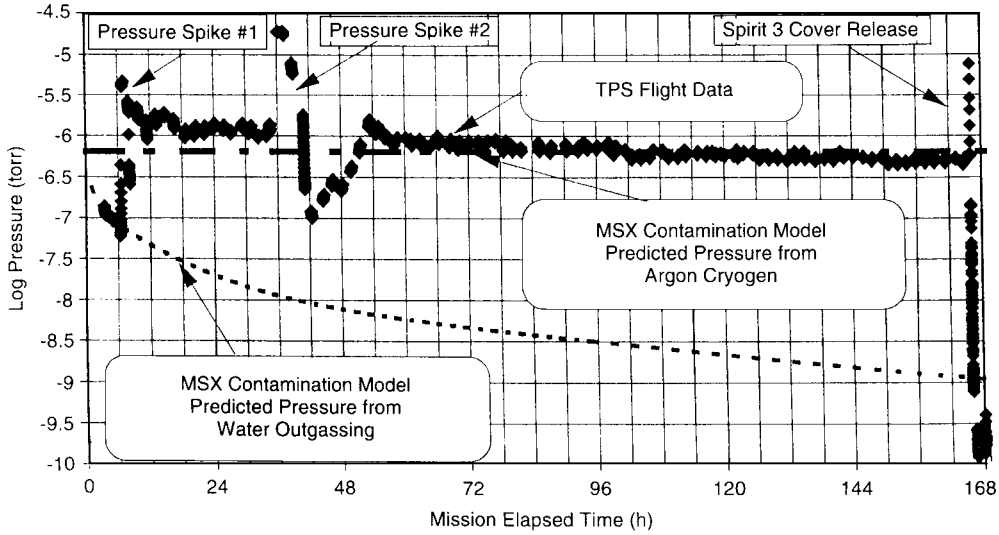

Fig. 2 TPS pressure data for the first mission week. Model prediction is also shown.

on and gathering data. Data from these instruments allowed us to make informed decisions about the advisability of optical sensor cover openings, particularly the SPIRIT III cryogenic sensor cover. The systematic trends observed by each contamination sensor during the first seven days on orbit are described next.

The TPS and QCMs were among the first science instruments provided power, and they began sending data only 1.45 h after launch. At 1.87 h mission elapsed time (MET), the pressure measured (which could contain some effect of TPS internal outgassing) was 2.2×10^{-7} torr. The spacecraft external pressure, even within this short period, had fallen below the regime of concern for external structure electrical arcing. The pressure fell below 10^{-7} torr by 3.5 h MET and continued to decrease after a time^{-1} decay. The magnitude and temporal trend agree well with MSX external contamination model predictions based on laboratory outgassing measurements for H_2O.[4]

The QCMs were powered on 1.45 h after launch. By 5 h after launch, the CQCM temperature had clearly decreased from its launch temperature, indicating that the cryostat vent to space had successfully opened and sublimation of the H_2 reservoir was occurring. The CQCM beat oscillation frequency was very stable and was observed to be at nearly the same value as before launch. Thus, no mass accumulation was observed due to redistribution through launch, and there were no vibration-induced leaks into the evacuated cryogenic optical telescope area. After we determined that the TQCMs were operating stably, we powered the Peltier coolers at 3.17 h after launch, and their temperatures dropped below $-40°C$ within 15 min.

Between 6.3 and 6.5 h MET, the pressure, measured by the TPS, increased from 5×10^{-8} to 8×10^{-7} torr, reaching 4×10^{-6} torr 30 min later. This increase was due to initiation of the release of argon vapor from the IR telescope door/cover. The solid argon in the SPIRIT III door was launched supercooled, and sufficient heating had occurred to produce the 8 lb of pressure required to cause the vent to open after 6 h in orbit. After opening, a pressure of argon emanating from the door venting was detected at about 10^{-6} torr levels, matching prelaunch predictions.[4] The TPS data for the first week are shown in Fig. 2. A second pressure burst (attributed to the vent remaining stuck open) was observed after 35 h MET. The NMS was operational during this second pressure burst and verified that the increase was due to argon exclusively.

Molecules

The TPS measures the total gaseous environment. MLI-covered spacecraft surfaces fill approximately 44% of the field of view. During the first week, the observed pressure is dominated by the argon vented from the SPIRIT III cover rather than by surface outgassing, as evidenced by the 75-fold pressure increase at the start of argon venting. The released argon flux undergoes self-collisions and is scattered into the TPS aperture. Aside from the pressure bursts,

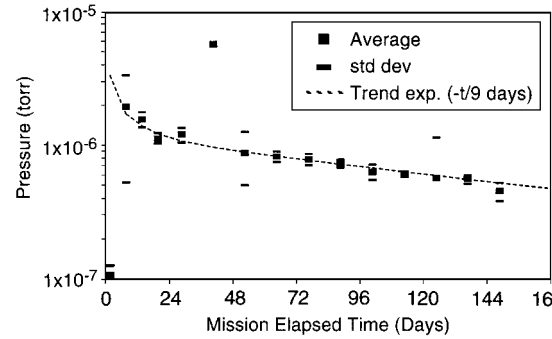

Fig. 3 Averaged TPS reading during argon venting. Exponential ($-t/9$ days) is shown for comparison.

the observed pressure decreased slowly over this period. All of the TPS readings averaged within a time period are presented in Fig. 3. Standard deviations are indicated to show the variability encountered during each period. (The TPS is calibrated and is expected to have an accuracy of greater than 25%.) The argon release is seen to follow a smooth exponential decay with a time constant of 9 days. A small (15%) additional early time (time^{-1}) contribution is required to match the data during the first day. The argon evolution decreases as the Dewar shell cools in orbit (reducing the heat load) and as the solid argon conduction paths to the door decrease.

During the early operations period, an additional trend within the argon decay is observed in both the TPS and NMS data. The observed TPS pressure oscillates periodically by about 25% in magnitude. A periodogram analysis[11] revealed the existence of a periodic frequency of this variation corresponding to once and twice per orbit. The source of this effect could be 1) return flux variations due to atmospheric variations (such as density increases) or 2) spacecraft heating.

The NMS provided insight into the constituents of the gaseous cloud during this period. The argon temporal trend matches the TPS observations. When argon venting began, it obscured the temporal decay of the outgassed species concentrations in the nondiscriminating TPS. The NMS $m/z = 18$ data clearly display the continued decay of the water vapor concentration in Fig. 4. Approximately 12% of the NMS field of view contains MLI, and the direct flux from the MLI surfaces was detectable. The pressures reported in Fig. 4 are corrected for the $^{36}Ar^{++}$ contribution to $m/z = 18$ and the noise background. After the first 45 h on orbit, the water-characteristic decay time changes from a time^{-1} to a time$^{-0.5}$ dependence. The data agree fairly well with the prelaunch predictions for the NMS geometry (also shown in Fig. 4).

The IMS was able to sporadically observe water ions produced by charge transfer with ambient atmospheric O^+. Because of the

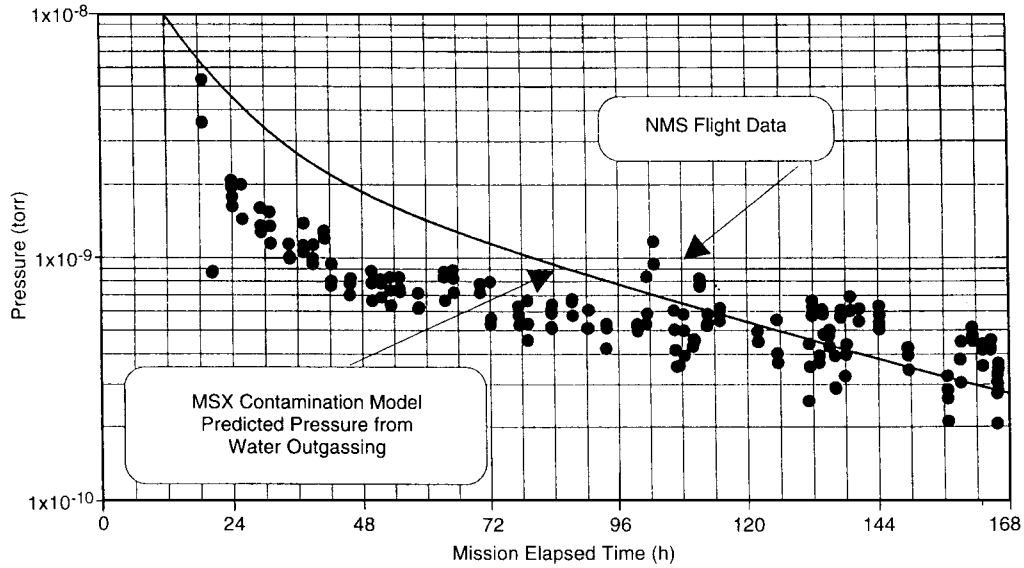

Fig. 4 NMS water observations during the first week. MSX model is shown for comparison.

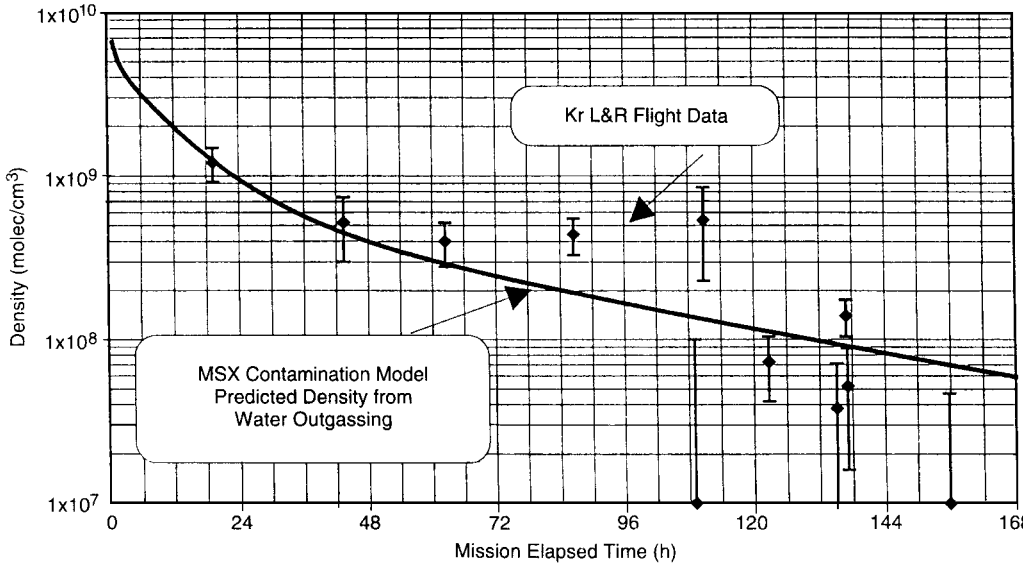

Fig. 5 KRF lamp and radiometer (Kr L&R) water measurements above MSX instrument section and model prediction.

complex interaction geometry, these data indicated that the process was occurring, but they were able to provide quantitative estimates of the local water density during early operations. The natural atmospheric and contamination data obtained by this instrument will be reported in future papers.

The KRF specifically measures the water concentration in a volume 50–100 cm above one corner of the 1.5-m^2 MSX instrument section.[12] Consequently, this water measurement represents an integral of the outgoing flux sources over the instrument section. Because of its high-power consumption during its 2-min measurement, the KRF is operated less frequently than the TPS and NMS. The 11 measurements performed during the first week are shown in Fig. 5. The preflight prediction of the expected levels at the KRF measurement volume is also shown and agrees with the general trend of the data. After an initial decay, very significant (factor of 100) variability is observed in measurements only a few hours apart. The variability is not correlated with the MLI or solar array temperatures in an obvious manner. The calibration of the lamps indicated an absolute accuracy of 25%, with a minimum detectable concentration of less than 10^7 water molecules per cm^3. Thus, the observed variability is believed to be real and not a simple temperature correlation. It has persisted for several months into the mission and will be discussed in future papers using a larger database to identify the variable water source on the spacecraft.[11,12]

Organics

The deposition of outgassed organic species was of great concern because of the sensitivity of UV optical instruments to attenuation even by films of nanometer thickness. Nearly all spacecraft materials were baked before assembly on the ground to reduce volatile condensible material outgassing. Mass spectra acquired at 24 h MET showed no obvious high mass species (between m/z 46 and 150). Twelve early-time spectra were averaged to establish a minimum detectable concentration of 6×10^{-12} torr or 2×10^5 molecules per cm^3 (three standard deviations). Later during the first week, the rear of the spacecraft ($-X$ face, electronics section) and the rear of the solar arrays that are usually shadowed were placed in direct sun to expedite molecular outgassing before cryogenic sensor opening. These surfaces are opposite the optical sensors and NMS fields of view. Forty-seven mass spectra obtained with the spacecraft in this configuration showed no increase in any mass number except 69. We have tentatively assigned this to CF_3 fragments (from trapped residual freon solvents). No statistically significant increase in water vapor or in any other mass was observed.

Within 3.4 h after launch, the four TQCMs were cold enough for accretion of organic species to occur, but they did not reach their final equilibrium values (near $-50°C$) until nearly 20 h after launch. The TQCMs point in different directions and have a wide 65-deg half-angle viewing field. Frequency changes occur when

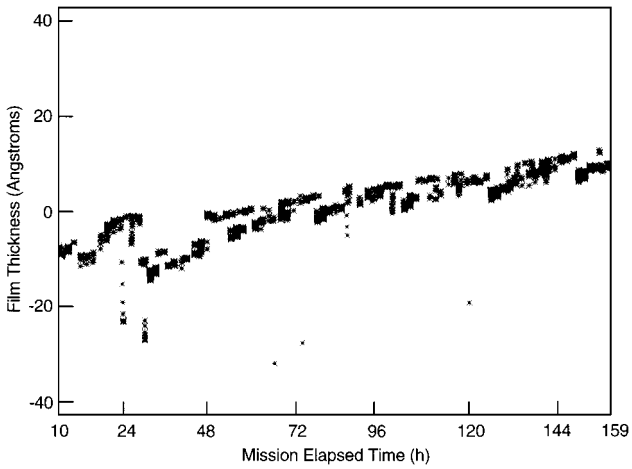

Fig. 6 TQCM 2 accretion measured from 2 h after launch until after SPIRIT III cover ejection.

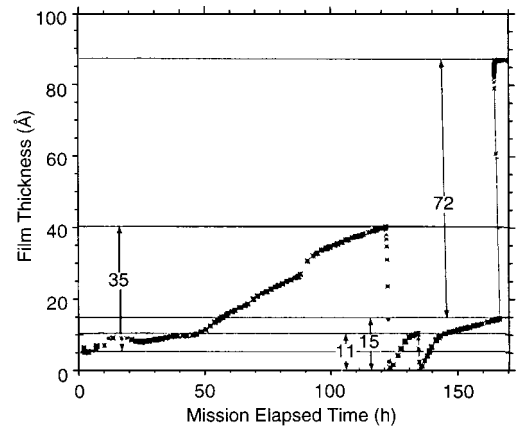

Fig. 7 Contamination film thickness observed on the CQCM as a function of time.

solar illumination produces thermal gradients in the TQCMs; however, molecular deposition can be distinguished from this thermal effect as the spacecraft maneuvers and moves around its orbit.

According to model predictions,[4] scattering by the argon cloud during the first week increases the return flux of these organic condensibles by nearly a factor of 100 above the nominal value of 10^{-6} expected at this altitude. If deposition had continued at this rate, degraded performance effects soon would have been observable on the solar arrays and thermal control system. After cover ejection, the deposition rate slowed significantly.

During the first week, TQCM 2 $(+Z)$ viewing the solar arrays had the largest deposition rate. The solar panels on MSX were subjected to thermal-vacuum bakeout for > 60 h at 90°C before launch. The TQCM frequencies recorded with minimum solar illumination are reported as film thickness in Fig. 6. Film thicknesses are relative to the value when the TQCM had reached its equilibrium temperature at 20 h MET. Thicknesses are calculated by assuming a film density of 1 g/cm^3. Just before the SPIRIT III cover release, a total of 1.2–1.4 nm of contaminant had deposited on TQCM 2 (≈0.2 nm/day). TQCM 1 pointed largely $-X$. As shown in Fig. 1, it thus has a view of the solar arrays, but it had a somewhat smaller accretion rate around 0.1 nm/day.

TQCM 3 $(+Y, -Z)$, wake viewing for most of the time, had very little accretion except for a discrete period at 60 h MET. Within a period of much less than an hour, the frequency increased by 50 Hz (1-nm-thick film). After that time, the frequency remained constant or slightly decreased during the rest of the first week in orbit. At 60 h MET, the edge of one solar array had a direct line of sight onto TQCM 3 and apparently deposited a film of thickness comparable to that accumulated on TQCM 1 and 2 during the entire first week. Thus, both cumulative exposure and even short-duration events can deposit films of thicknesses that produce optical attenuation in the UV. Attention to details at this level is required during mission operations planning to prevent optical system degradation.

TQCM 4 dominantly faces $+X$ along the optical axis of the primary sensors and was positioned to have no direct view of any spacecraft surfaces. Significant accretion levels may indicate primary sensor accumulation. Between 24 and 90 h MET, a 0.4-nm-thick film was deposited, a level sufficient to cause concern for the UV sensor. Thus, before opening the UV sensor protective cover, we performed a real-time diagnostic experiment to assess the impact of this deposition rate on the UV optics. The TQCM crystal surface was briefly heated at 95 h MET from its operational temperature of −50 to −15°C (the temperature of the primary mirrors in the UV spectrometers and imagers). Over 60% of the mass deposited on TQCM 4 promptly evaporated during this process. The vapor pressure of these molecules was sufficient that they would not have accumulated on the warmer UV optical surfaces. Because the TQCM crystals were held at −15°C for only a few minutes, additional mass may have evolved more slowly. Also, TQCM surfaces are solar illuminated, and photolytic polymerization may induce conversion of volatile molecules accreted at −50°C into permanently deposited high-molecular-weight chain species.[13] Thus, the 40% of TQCM 4 film remaining after heating was believed to be a large overestimate of the mass deposition rate that would have occurred on the UV optical surfaces (which are never solar illuminated). Thus, based on these observations and the modeled cover opening safety criteria, we advised the planning team that it was safe to open the UV sensor covers.

Cryogenic Film Deposition

The solid-argon-filled Dewar covering the aperture at launch formed the vacuum seal as well as reducing the radiative load on the Dewar and acting as a getter for water (and organic) molecules during ground processing and launch. However, if the cover warmed above 150 K before deployment, the molecules frozen on the door would have a direct line of sight to the primary mirror and CQCM. The early operations period duration is a balance between allowing the external environment to decay to a level permitting safe operation and the lifetime of the cryogen in the aperture cover. The CQCM inside the SPIRIT III cryogenic Dewar near the primary mirror provided a continuous monitor of the primary mirror temperature and accretion. Redistribution of condensed gases will occur as the temperature gradients inside the Dewar and telescope change from ground values and with operations in orbit.

The deposited frozen film thickness on the CQCM during the first week after launch is shown in Fig. 7. Again, a film density of 1 g/cm^3 is assumed, yielding a value of 22.6 Hz per nanometer of thickness.[7] On two occasions during this period, the CQCM crystal was heated to 40 K at a controlled rate of 1 K/min. The same oscillation frequency was obtained after each heating and was taken as the reference for zero film thickness. There was a deposition of 0.7 nm from the time of the last preflight measurement until the first orbital contact. The cumulative deposition from first contact until cover ejection was an additional 6.1 nm.

A thermogravimetric analysis (TGA) was performed on the CQCM at 121 and 134 h MET. Analysis of the frequency change during the CQCM TGA warming cycle provides a measure of mass fraction removed as a function of temperature. Essentially all of the deposition evaporated between 26 and 34 K, with the peak rate at 31 K. Based on controlled laboratory experiments[14] and ground testing,[15] we identified the deposited material as mainly molecular oxygen, O_2, arising from the redistribution of atmospheric oxygen condensed during prelaunch cryogenic cooling.

Particles

Particles can reduce optical sensor performance by depositing on sensitive surfaces, increasing scattering, and by obscuring or distorting far-field optical scenes. Particles originating from the spacecraft can be detected across the UV to IR spectrum by their thermal emission, scattered sunlight, and earthshine. The XEF operating in conjunction with a 10.5 × 13.1 deg IVW permits quantitative particle measurement in a volume centered 2 m above the spacecraft under conditions independent of external illumination levels. Particles are illuminated with 400- to 900-nm light in a series of nine

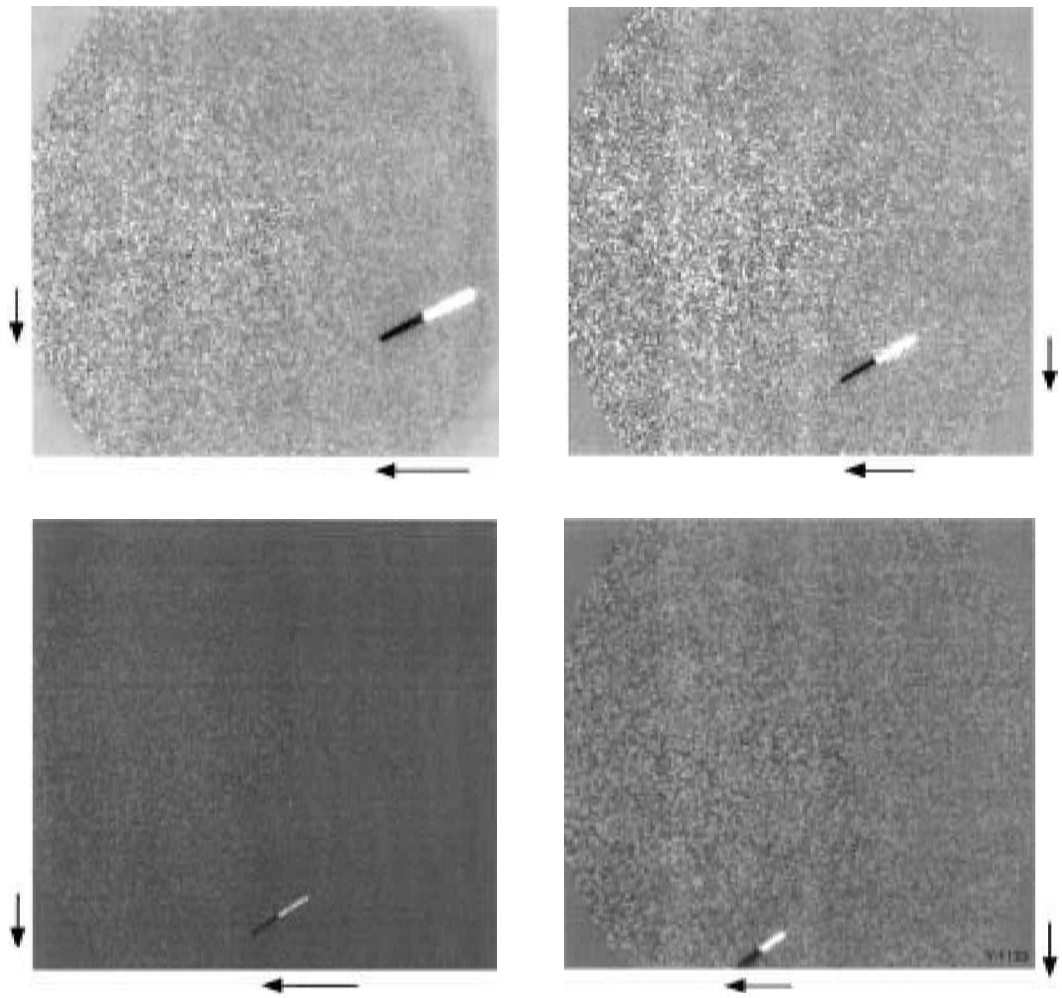

Fig. 8 Sequential images of a single particle observed after a termination crossing at 123 h MET.

11-ms pulses sequenced to permit velocity determination within a single image.[6,16] During the first week in orbit, the particulates observed are likely residual from ground operations as brought to orbit with the spacecraft.

Although particles were clearly observed associated with discrete operational events (as described in the next section), particles were observed even during spacecraft passive periods. At the 904-km altitude of MSX, atmospheric drag effects are small and particles can remain in the fields of view of the optical instruments for long periods. Particles were observed to remain in the IVW field of view for over 200 s. Several data-collection events were scheduled at different positions around the orbit to isolate production processes. At 123 h MET, the spacecraft was maneuvered to a constant attitude ($+X$ 50 deg to the sun vector) several minutes before umbra exit. The spacecraft MLI surfaces had already undergone many insolation cycles. (This was during the 72nd orbit.) Particles were detected in 5.5% of the images obtained as the spacecraft passed from orbital night into solar illumination. The sequential images of one of these particle's trajectories is shown in Fig. 8. The particle in this image is at 200 cm and has a velocity vector of 20 cm/s relative to the spacecraft. Mapping of the trajectories backward indicates that the particles originated on the $+X$ face of the spacecraft at a time just after solar illumination.[16] A particle also was observed moving toward the spacecraft with a 30-cm/s velocity vector. This particle also could have originated on MSX re-entering the field of view after being released on an initial trajectory downward in the direction of satellite motion, "ram." Thus, atmospheric drag will decelerate the particle relative to the spacecraft and cause it to sweep back toward the spacecraft. The MSX external contamination model has shown which ranges of sizes, release velocities, and directions will lead to trajectories that reencounter the spacecraft.

Discrete Events

SPIRIT III Aperture Cover Venting

The solid argon cooling the SPIRIT III aperture door vented through two redundant spring-loaded valves, creating the argon cloud surrounding MSX. The initial pressure burst at 6.5 h MET was observed only by the TPS (Fig. 2). After the NMS was turned on, a second burst was observed after 35 h MET by both TPS and NMS. The NMS measures the absolute argon partial pressure, as shown in Fig. 9. The pressure increase produced by the venting was observed for approximately 6 h. We believe that the argon vent was stuck open because of frozen material, redundant valve competition, or mechanical effects.[11] A result of this extended venting is cooling of the SPIRIT III cover by 6°C during the extended release period in response to gas expansion cooling and argon boiling-point depression. Once the venting stopped, the cover temperature stopped cooling and continued its upward trend. The vented argon concentration surrounding the spacecraft as monitored by the TPS and NMS remained at reduced levels for the next 12 h, until the cover temperature returned to the level of its long-term trend.

Optical Sensor Door Openings

The XEF was operated during periods of mechanical operations, such as all sensor door opening and cover release events. In spite of the careful ground operations procedures to minimize particulate levels, particles associated with every one of these events were detected. An image acquired by the IVW 20 s after its hinged cover opening contained approximately 20 particles. The particles were observed via scattered sunlight (125 deg to $+X$). To protect the image intensifier, the gain was relatively low for this image. The particles have similar trajectories: away from the spacecraft with a large velocity component along the direction of cover motion and

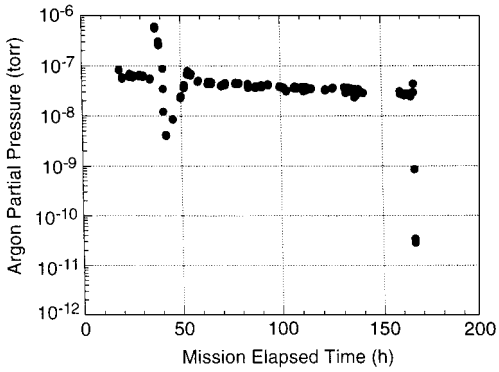

Fig. 9 Argon density measured by the NMS from 20 until 200 h MET.

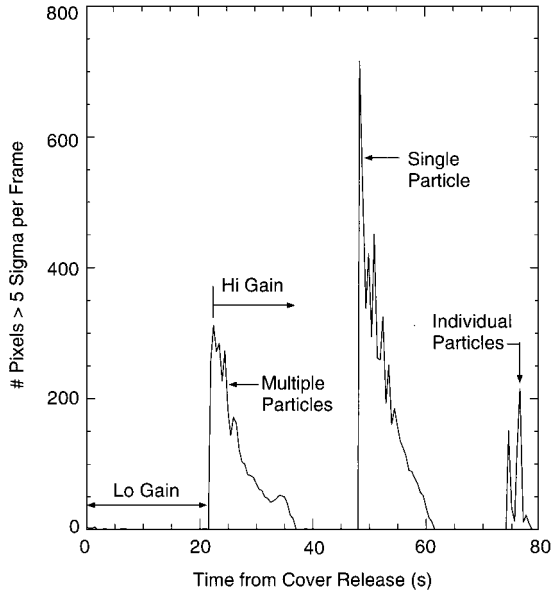

Fig. 10 Temporal decay of pixels per frame exceeding 5 standard deviations in brightness after IVW door opening.

a smaller perpendicular velocity. Similar particle densities and trajectories were observed associated with every sensor door opening.

Although the optical environment was severe during door openings, the particles cleared quickly. The observed temporal dependence of the particles detected in the IVW images after its own cover opening is shown in Fig. 10. Gain was changing during this period, confounding exact analysis, but several trends were observed. As the gain increased, particles became observable 20 s after the opening. Between 20 and 40 s, multiple near-field particles were detected in each frame. Particles near the spacecraft were out of focus, and their image produced a blurred circle. This blurred particle image added significant (five times the dark noise) signal onto over 300 pixels (roughly a 0.5 × 0.5 deg angular portion of the image). Between 48 and 62 s, a single (very large) defocused particle slowly transited the image, contributing radiance to over 700 pixels in each image. Later in time (at 74–78 s), other single particles were detected. At 90 s, the imager switched to a far-field focus. A single particle was observed in-focus moving through the field of view at distances in excess of 65 m. In these data and during other cover openings, most particles have moved out of the field of view of the IVW sensor in less than a minute. At later times, straggling particles were nearly always observed but represented a nuisance rather than a threat to accurate measurement sequences.

SPIRIT III Cover Ejection

The IR sensor system is required to perform observations with high off-axis rejection. The level of scattered radiation is an extremely sensitive function of particulate contamination levels on the cryogenic primary mirror.[15] Because significant particle generation was expected and observed with all mechanical cover openings on MSX, we planned to open the SPIRIT III cover after all other systems had been operated in orbit. This delay also permitted molecular outgassing to decay to lower levels.

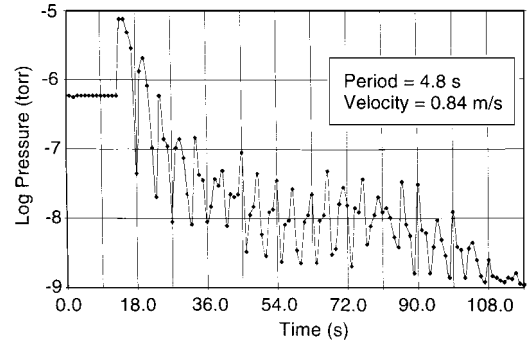

Fig. 11 TPS pressure measurements during SPIRIT III cover ejection showing recession and rotation.

The release of the SPIRIT III cover marked the end of the early operations period and the start of the cryogenic operations period. Based on modeled cover opening safety criteria, the contamination team advised operations that it was safe to remove the SPIRIT III cover by 108 h MET. Because the temperatures of the argon cryogen cooled cover were still in the acceptable range, the release was performed as planned at 165.95 h MET (slightly less than seven days after launch).

The SPIRIT III cover (100-kg mass, ≈0.5-m diam) requires a release mechanism with pyrotechnic actuators. Thorough ground testing of the sealed pyrotechnic devices demonstrated that only very small quantities of gases (mainly CO_2) were released. Upon actuator release, springs force separation and rotation of the cover. Release occurs after rotation to 30 deg from the optical axis. Based on ground testing, the cover was predicted to move away from MSX at a velocity of 0.74 m/s after ejection, rotating about its center of gravity once every 3–4.2 s. We were able to observe the effects of cover opening in the data from several instruments.

The TPS data from the period after cover ejection are shown in Fig. 11. The door opening time is clearly marked by a pressure increase as the cover moves into the TPS field of view. The ambient pressure surrounding the spacecraft drops by almost 3 orders of magnitude within the first 3 min after release to a value below 10^{-9} torr, i.e., after the argon venting source is removed, the pressure rapidly decays to below the predicted level expected from residual outgassing; see right-hand side of Fig. 2. The pressure oscillation caused by cover rotation is reproducible and implies a rotation period of 4.8 s. Analysis of the pressure decrease[11] derived a velocity away from the spacecraft of 0.84 m/s, in excellent agreement with expectations.

The cover continues to vent argon as it tumbles away from MSX, and some of these atoms reach the primary IR mirror within the SPIRIT III telescope. The CQCM detected a 7.2-nm increase in accreted mass during this cover release, as shown in Fig. 7. The magnitude of this increase is very consistent with the integrated pressure history observed by the TPS during cover release. A TGA was performed several weeks after cover release. The mass evolved from the CQCM at temperatures indicating that this entire deposit was likely argon. Based on prelaunch laboratory measurements of cryogenic mirror performance degradation,[10] the changes in mirror properties resulting from the molecular deposition measured on the CQCM during the first week and during cover ejection are considered insignificant.

The shock from the pyrotechnic actuators imparted momentum to the spacecraft and resulted in the release of many particles from spacecraft surfaces. These dislodged particles are probably from ground operations and brought to orbit on MSX surfaces. The dislodged particles are observed with the primary optical sensors by UVISI and by SPIRIT III itself.

Three sequential frames for the UVISI IVW imager are shown in Fig. 12. They were taken just after the time of the SPIRIT III cover release and were separated by 0.5 s. The optical environment is very severe at this time, with an optical transmission to the far field near zero. Particle velocities extracted from the pulsed illumination are

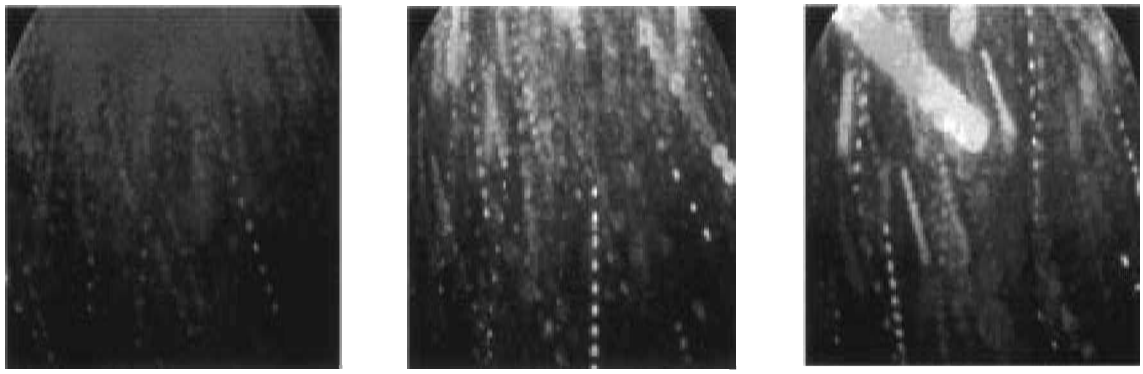

Frame 63 Frame 64 Frame 65

Fig. 12 IVW imager data frames 0.5 s apart from time of SPIRIT III cover ejection. Particles in the meter-per-second range are observed.

on the order of meters per second. The first objects observed by the IR radiometer arrays were the bright near-field tracks of particles from its cover release. Radiance from up to nine out-of-focus particles were detected in the first image. Shortly after the SPIRIT III cover release, MSX maneuvered its optical axis away from the receding cover. Within 2.5 min, particles were no longer observable in the UVISI IVW images. Although previous IR radiometric space observations of particles indicate that they should be observable out to distances of many kilometers,[8] particle tracks were no longer observable 10 min after cover release. Thus, the cover-induced particles rapidly move away from MSX and out of the field of view.

Conclusions

The contamination instrument data have been shown to be useful for making informed decisions about spacecraft operations and primary sensor performance. We have demonstrated the ability to provide near-real-time responses to operational issues. This rapid response permitted assessment of primary optical sensor performance and prioritization of various activities. The information provided by our instruments permitted the primary sensors to become operational as soon as possible without compromising their performance. This saved efforts by the operations team in contingency planning (and replanning) time. The TPS proved to be particularly valuable during early operations by providing high-time-resolution data. The CQCM sensed the total integrated film thickness deposited near a location of critical concern—the SPIRIT III primary mirror. The CQCM provided continuity from ground operations that provided confidence that the optical sensor performance had not suffered performance degradation from its prelaunch level until after cover opening in orbit because of film deposition.

At the end of the MSX early operations period, the contamination instruments indicated that 1) SPIRIT III optical surfaces suffered negligible performance degradation from their prelaunch levels because of molecular film deposition; 2) the UV/visible sensors suffered negligible performance degradation because of molecular film deposition from the external environment surrounding the spacecraft; and 3) it was safe to initiate the mission measurements plan with only occasional interference (at an acceptable level) from gaseous or particulate contamination.

The contamination instruments verified that careful material selection and ground assembly procedures resulted in a spacecraft that could be ready to perform sensitive optical measurements on orbit after a short predictable period for outgassing. The contamination instruments validated the MSX external contamination model predictions. Such validated models will be a valuable asset to future space systems designers. We recommend that a reasonable cost-effective contamination control plan and contamination model become standard tools in future spacecraft design. A more complete assessment of the contamination control plan and its effectiveness will be done after the long-term environment has been measured.

Acknowledgments

The authors gratefully acknowledge many useful discussions with Ray Russell, Paul Griffith, Jim Dyer, Russ Cain, the MSX Operations team, and Lt. Col. B. Guilmain (the MSX Program Manager at the Ballistic Missile Defense Organization).

References

[1]Mill, J. D., O'Neil, R. R., Price, S., Romick, G. J., Uy, O. M., Gaposchkin, E. M., Light, G. C., Moore, W. W., Jr., Murdock, T. L., and Stair, A. T., Jr., "Midcourse Space Experiment: Introduction to the Spacecraft, Instruments, and Scientific Objectives," *Journal of Spacecraft and Rockets*, Vol. 31, No. 5, 1994, pp. 900–907.

[2]Paxton, L. J., Meng, C.-I., Anderson, D. E., and Romick, G. J., "MSX—A Multi-Use Spacecraft," *Johns Hopkins University APL Technical Digest*, Vol. 17, No. 1, 1996, pp. 19–34.

[3]Silver, D. M., "Midcourse Space Experiment Contamination Modeling," AIAA Paper 96-0223, Jan. 1996.

[4]Silver, D. M., "Midcourse Space Experiment: Early Flight Molecular Contamination Modeling Predictions," AIAA Paper 97-0839, Jan. 1997.

[5]Glassford, A. P. M., and Garrett, J. W., "Characterization of Contamination Generation Characteristics of Satellite Materials," Lockheed Missiles and Space Co., WRDC-TR-89-4114, Sunnyvale, CA, Nov. 1989.

[6]Uy, O. M., Benson, R. C., Erlandson, R. E., Boies, M. T., Lesho, J. C., Galica, G. E., Green, B. D., Wood, B. E., and Hall, D. F., "Contamination Experiments in the Midcourse Space Experiment," *Journal of Spacecraft and Rockets*, Vol. 34, No. 2, 1997, pp. 218–225.

[7]Wood, B. E., Hall, D. F., Lesho, J. C., Dyer, J. S., Uy, O. M., and Bertrand, W. T., "QCM Flight Measurements of Contamination on the MSX Satellite," *Proceedings of the SPIE*, Vol. 2864, Aug. 1996, pp. 187–194.

[8]Green, B. D., Mulhall, P. A., Rawlins, W. T., and Uy, O. M., "Optical Signatures of Particles in Space," *Optical Engineering*, Vol. 37, No. 1, 1997, pp. 56–72.

[9]Cranmer, J. H., Sanders, J. T., Jr., Lesho, J. C., and Uy, O. M., "Contamination Control for the Midcourse Space Experiment: An Overview," *Johns Hopkins University APL Technical Digest*, Vol. 17, No. 1, 1996, pp. 88–101.

[10]Sieber, B. L., Bryson, J. R., and Wood, B. E., "Cryogenic BRDF Measurements at 10.6 μm on Contaminated Mirrors for the MSX Satellite Program," *Proceedings of the SPIE*, Vol. 2261, July 1994, pp. 170–180.

[11]Boies, M. T., Phillips, T. E., Silver, D. M., El-Dinary, A. S., Uy, O. M., Dyer, J. S., and Mill, J. D., "Total Pressure Sensor Results from the Early Operations Phase of the MSX Mission," *Proceedings of the SPIE*, Vol. 2864, Aug. 1996, pp. 138–156.

[12]Galica, G. E., Atkinson, J. J., Aurilio, G., Shepherd, O., Lesho, J. C., and Uy, O. M., "Optical Measurements of the MSX Local H_2O Density," *Proceedings of the SPIE*, Vol. 2864, Aug. 1996, pp. 181–186.

[13]Stewart, T. B., Arnold, G. S., Hall, D. F., Marvin, D. C., Hwang, W. C., Young Owl, R. C., and Marten, H. D., "Photochemical Spacecraft Self-Contamination: Laboratory Results and Systems Impacts," *Journal of Spacecraft and Rockets*, Vol. 26, No. 5, 1989, pp. 358–367.

[14]Bryson, R. J., Bailey, A. B., Sieber, B. L., Bertrand, W. T., Jones, J. H., and Wood, B. E., "CQCM: Characterization and Calibration for MSX," *Proceedings of the SPIE*, Vol. 1754, July 1992, pp. 205–214.

[15]Dyer, J. S., Mikesell, R., Perry, R., Mikesell, T., and Guregian, J. J., "Contamination Measurements During Development and Testing of the SPIRIT III Cryogenic Infrared Telescope," *Proceedings of the SPIE*, Vol. 2261, July 1994, pp. 239–253.

[16]Galica, G. E., Green, B. D., Atkinson, J. J., Aurilio, G., Shepherd, O., Lesho, J. C., and Uy, O. M., "Flashlamp Measurement of the MSX Particulate Environment," *Proceedings of the SPIE*, Vol. 2864, Aug. 1996, pp. 169–180.

R. G. Wilmoth
Associate Editor